(sciencefront.org) ISSN 2394-3688

Misalignment studies in laser diode to hemispherical microlens tipped circular core photonic crystal fiber excitation

Sumanta Mukhopadhyay

St. Paul's Cathedral Mission College, Department of Physics, 33/1 Raja Rammohan Roy Sarani, Kolkata-700009, West Bengal, India.

Corresponding author E-mail: sumukherjee_74@yahoo.com

(Received 17 September 2017, Accepted 02 November 2017, Published 14 November 2017)

Abstract

We investigate theoretically the coupling optics involving a laser diode and a series of circular core photonic crystal fibers with different air filling ratio and hole-pitch via hemispherical microlens of allowable aperture on the tip of such fiber in absence and presence of possible transverse and angular misalignments. By employing Gaussian field distributions for both the source and the fiber and also the already derived ABCD matrix for hemispherical microlens, we formulate analytical expressions for the concerned coupling efficiencies for practically interesting two different light emitting wavelengths of 1.3 μm and 1.5 μm, respectively. Further, it is observed that, for a fit radius of curvature of 6.0 μm of hemispherical microlens, photonic crystal fiber with air filling ratio of 0.45 and hole-pitch of 4.5 μm comes out to be the most suitable one to couple laser diode emitting light of wavelength $\lambda = 1.3\mu m$. Moreover, the coupling efficiency can reach to 86.88% with simultaneous optimization of radius of curvature and working distance of specific lensed fiber. Such analysis which as per our knowledge is the first theoretical investigation, will be extremely important in ongoing investigations for the design of optimum launch optics involving hemispherical microlens on the tip of photonic crystal fiber. Moreover, the results are extremely useful for assessing deeply the sensitivity of such coupler with reference to above kinds of misalignments.

Keywords: ABCD matrix, Circular core photonic crystal fiber, Optical coupling, Transverse misalignment, Angular misalignment

1. INTRODUCTION

Photonic crystal fibers (PCFs), also known as microstructured optical fibers, have attracted a considerable amount of attention recently, because of their unique properties that are not realized in conventional optical fibers (COFs). PCF is actually a unique type of pure silica optical fiber

[1-3] with an array of air holes running along the total length of the fiber, reminiscent of a crystal lattice, which gives to this type of fiber, its name. The core is formed by omitting the central air hole of the structure (Fig. 1). Depending upon the light-guiding mechanism, PCFs can be categorized into two main classes. The first one, air-guided hollow core PCFs in which light is guided by the photonic band-gap (PBG) effect, a mechanism that does not need a higher refractive index in the core for the confinement and guidance of light provided the frequency of the light is in the bandgap of two-dimensional photonic crystal formed by the periodic cladding. Different kinds of band gap PCFs such as all solid, low loss air core, have been also designed which find important applications that include CO_2 laser beam transmission, gas sensing, etc.[4].

On the other hand, the second one, index-guided solid core PCF for which the lower effective refractive index of the surrounding holes creates the cladding and the light is confined to the central solid core as in COFs and guided by modified total internal reflection (MTIR) mechanism. The index-guiding fiber, has a solid core region surrounded by a solid silica cladding, with regularly arranged air holes in a periodic arrangement, whose effective refractive index depends on the ratio of air to glass, also known as the air-fill ratio that comprises the structure. The presence of the holes in the cladding region leads to the reduction in the effective refractive index of the cladding region, which will provide the variation of refractive index necessary to support total internal reflection at core cladding boundary. Therefore, the light is confined to the solid silica core, which has a relatively higher index than the effective cladding refractive index [4, 5]. Because of high design flexibility of the PCFs compared to COFs, important optical properties can be tailored in PCFs [4, 5]. For index guiding solid core PCFs, these properties include endlessly single modeness, high numerical aperture, large mode area, high nonlinear coefficient, high birefringence and tailorable large dispersion [4]. Moreover, PCFs can transport light with very low loss in certain wavelength where COFs possess very large loss [5].

Now, the preservation of polarization state of the optical field, which is an essential feature in coherent optical communications and in some specific fiber-optic sensors, can be maintained by introducing modal birefringence. In optical fibers, birefringence can be achieved either by introducing stress in the fiber profile or by creating asymmetry in the core region. However, achievable birefringence is small in COFs due to the small index difference between core and cladding while high birefringence can be easily achieved in PCFs due to the large index contrast between core and cladding. The key technique is to destroy the symmetry of the structures of core and cladding. The structural symmetry of the core and cladding can be destroyed either by changing the shape or the size of the air holes near the core region or by changing both [4, 5]. Though the band gap PCF promises very large birefringence (~$5.45\text{x}10^{-2}$) at 1.55 μm [4], the birefringence of the index guided PCF yields also a very large value (~2.22×10^{-2}) [5] at same wavelength of light**.** Such high value of birefringence will be useful for making these fibers attractive in the fabrication of different fiber optic sensors such as humidity, strain, pressure, temperature, acoustic wave, etc. as well as in the fabrication of polarization controllers [4, 5]. Moreover, band gap PCFs may be also useful in optical communications [4]. Bhattacharya

and Konar have investigated a new type of index-guided PCF having triangular lattice of air holes which can be used for spectroscopy, biomedical application, and supercontinuum generation [6]. Sharma et al. [7] have proposed a PCF which provides a large optical nonlinearity and moderate dispersion simultaneously, thereby their proposed PCF can act as a very efficient nonlinear medium for supercontinuum generation. The interest in supercontinuum generation is driven by several important applications such as optical metrology, optical coherence tomography, spectroscopy, frequency comb generation and wavelength division multiplexing [7]. Thus, in view of a wide range of optoelectronic applications of PCF in different sectors, the study of this special kind of optical fiber is of tremendous importance [8].

An efficient coupling between laser diodes (LDs) and single-mode fibers (SMFs) is one of the most fundamental, important technical aspects in the construction of practical fiber transmission networks employing erbium-doped optical fiber amplifiers (EDFAs) and it is always the hot investigative field in recent years. Actually, a wide range of optoelectronic integrated semiconductor devices needs highly efficient, low-loss coupling which requires a gradual spot size transformation of the laser mode for the better compatibility of the wavefront and spot size of the laser beam to those of the guided mode in the fiber. Thus, optical packaging of semiconductor LD requires high coupling efficiencies and large misalignment tolerances from the viewpoint of its application based orientation for making the devices more rugged, more reliable and easier to handle. The fabrication of different integral microlenses on the tip of the fiber is the most popular scheme for improving the coupling efficiency. Moreover, the advantage of alignment free and miniature optical design between the microlens and the fiber, demands the development of microlens on the tip of the fiber. The advantage of the design of more-compact optical components and modules also makes the fabrication and design of fiber microlens vitally attractive. Benefit of fiber sensing and optical recording also demands the use of fiber microlenses [9]. These microlenses, whether conical or hemispherical, possess the advantage of being self-centred. Such microlenses may have hyperbolic, hemispherical, parabolic, elliptic, upside down tapered surfaces to modulate the spot size of LD light incident on them and transmit it into the SMF [10-27].

Another important study in microlens coupling scheme includes losses due to possible types of misalignments, in between laser and fiber spot sizes, which cannot be avoided due to practical difficulties occurred during the formation of the microlens on the tip of the fiber instead of being capable of forming it precisely at the ideally set position as shown in Fig. 1. Therefore, one cannot avoid the possible mismatches, as in conventional splicing of two fibers [28]. Further, the limitations of fabrication of the said type of coupler may lead to relative shift between the microlens output and the fiber input faces resulting in two kinds of possible misalignments, namely, transverse and angular misalignments. Thus, the losses are also incurred due to two kinds of misalignments while we couple light via microlens through a SMF. Such investigation is important and pertinent for assessing the sensitivity of the efficient coupler in the presence of two types of misalignments.

Now, the ABCD matrix technique has been widely used in analyzing and designing microlenses of different types of conic sections on the tip of the fiber as far as coupling of a LD with SMF is concerned. These ABCD matrix treatments are elegant not only due to their simplicity but also for their predictability of such coupling efficiencies accurately with very little mathematical calculations. It may be relevant to mention in this connection that the coupling optics involving hyperbolic microlens on the tip of the circular core step index single mode fiber (CCSISMF) [14-16] as well as on the tip of circular core graded index single mode fiber (CCGISMF) [17] in absence and presence of possible transverse and angular misalignments have been previously reported based on respective ABCD matrix formalism [14, 15]. Moreover, the coupling optics involving hemispherical microlens (HEML) on the tip of CCSISMF [18, 19] as well as on the tip of CCGISMF [20] have also been already reported based on relevant theoretical ABCD matrix model [18]. The coupling optics involving parabolic microlens on the tip of CCSISMF [21, 22] as well as on the tip of CCGISMF [23] have been recently reported based on very popular and relevant ABCD matrix formalism [21, 22]. Based on the prescribed transformation ABCD matrix of another novel and popular type microlens like upside down tapered microlens [25, 26], the studies of the coupling losses in absence and presence of possible transverse and angular misalignments in case of LD to CCSISMF [26] as well as on CCGISMF [27] coupling via upside down tapered microlens on the tip of such fibers have also been already reported.

Thus, in the context of coupling optics there are enormous amount of research works on microlenses like hyperbolic, hemispherical, parabolic microlenses etc. on the tip different types of circular core COFs which have enriched the literature [10-27]. However, as per as research and developments associated with microlensing coupling schemes on the tip of circular core photonic crystal fibers (CCPCFs) are concerned, only a research paper investigating coupling of LD to solid core PCF via hyperbolic microlens has been reported very recently [29]. Moreover, no such information is available regarding a study of coupling optics involving LD and CCPCF via HEML on the tip of such fiber in presence of possible transverse and angular mismatches. Actually the formation of HEML on the end of an optical fiber is most promising because of its relative ease of fabrication using simple photolithographic technique, reasonable coupling efficiency and reduced harmful back reflected light into the LD [11, 12, 18]. Thus, our aim is to study the coupling losses in absence and presence of possible transverse and angular misalignments in the case of a LD-to-CCPCF coupling via a HEML on the tip of such fiber.

In the first part of this paper, we theoretically investigate the coupling efficiencies between a semiconductor LD emitting light of wavelength $\lambda = 1.3\ \mu m$ [12] and a series of CCPCFs with different air filling ratio d/Λ and lattice constant or hole pitch Λ [29] via HEML of two different radii of curvatures [18, 19] on the tip of these fibers in absence of possible transverse and angular misalignments. In the second part, we carry out the similar investigation for a LD emitting light of wavelength $\lambda = 1.5\ \mu m$ [12]. A comparison between these two cases is performed. Finally, the transverse and angular misalignments are studied for the most suitable fiber having a specific air filling ratio d/Λ and lattice constant or hole pitch Λ excited with two

LDs emitting light of a particular wavelength. As stated earlier, this analysis is based on previously derived simple ABCD matrix for refraction by a HEML [18, 19]. In fact, predictions of coupling optics by ABCD matrix formalism have produced excellent results as far as coupling of LD via HEML of specific radius of curvature on the tip of CCSISMF [18, 19], and CCGISMF [20] are concerned. Concerned calculations need very little computations.

Further, we employ Gaussian field distributions for both the LD and the fiber. Experimentalists, system engineers and packagers would find these results appealing in designing CCPCFs with appropriate calibration, in the context of its simplicity in comparison with other deeply involved rigorous methods like finite difference method (FDM) and finite element method (FEM). The present analysis, reported for the first time, contains significant new results in connection with the prediction of the suitable optogeometry of the HEML as well as that for the appropriate design of fiber geometry, i.e., core size, the air hole size, air hole pitch and the distribution of air holes, at a suitable wavelength emitted from the source. The results should be extremely important for the designers and packagers who can, accordingly, mould and shape the desired HEML at the CCPCF for achieving optimum coupling optics involving CCPCF in which air hole size, pitch, and distribution are additional degrees of freedom in comparison with the COFs. Moreover, the results are extremely useful for assessing deeply the sensitivity of such coupler with reference to above types of mismatches.

2. THEORY AND ANALYSIS

2.1. Preview of fiber spot sizes of CCPCF

In our study, we consider an all-silica CCPCF with a triangular lattice of uniform structure for the air-hole of diameter d and glass matrix elongated along the total length of the propagation direction of the fiber, as shown in Fig. 1. The air-holes are distributed symmetrically around a central silica defect, which is actually an omitted air-hole, acting as the core of the said CCPCF. The infinite air-hole matrix with lattice-constant or hole-pitch Λ and air filling ratio d/Λ has been considered to act as the cladding of the CCPCF. Since the core-index n_{CO} is greater than that of the effective cladding index n_{FSM}, the fiber can guide light by the mechanism of MTIR as in case of a conventional step index fiber (CSF) [29, 30].

Now, the fundamental modal field in a CCPCF is approximated as a Gaussian function [29, 31] in the single mode region where air filling ratio of the PCF is smaller than 0.45 [32]

$$\psi_f = \exp\left[-\frac{x^2 + y^2}{w_{eff}^2}\right] \tag{1}$$

where w_{eff} corresponds to the spot size of the CCPCF.

The upper and lower limits of the propagation constants β of the guided modes through the core of the CCPCF satisfy [8, 30]

$$k n_{CO} > \beta > \beta_{FSM} \tag{2}$$

where, $k=2\pi/\lambda$ being the wave number associated with the operating wavelength λ, n_{CO} is the refractive index of silica or the core material and β_{FSM} is the propagation constant of the fundamental space-filling mode (FSM), which is the fundamental mode in the infinite photonic crystal cladding without any defect or core.

The index corresponding to the FSM or the effective cladding index is [8, 30]

$$n_{FSM} = \frac{\beta_{FSM}}{k} \tag{3}$$

The procedure for obtaining the value of n_{FSM} for given parameters of the CCPCF at operating wavelength of light is detailed in Appendix A [29, 30]. Here all the coefficients are determined by applying the least square fitting method for practically interesting two operating wavelengths $\lambda = 1.3\mu m$ and $\lambda = 1.5\mu m$, presented in Tables 1 and 2, respectively. These coefficients are utilized to determine the values of n_{FSM} of the CCPCF for various values of hole-pitch and the air filling ratio at any particular wavelength of interest [29].

Table 1

Values of all coefficients required for the formulation of effective cladding index n_{FSM} at $\lambda = 1.3\mu m$.

$\lambda = 1.3\mu\, m$			
	$i = 0$	$i = 1$	$i = 2$
A_i	1.430434	0.003803	-0.000214
B_i	0.069387	-0.012541	0.000650
C_i	-0.375746	0.107635	-0.008799

Table 2

Values of all coefficients required for the formulation of effective cladding index n_{FSM} at $\lambda = 1.5\mu m$.

$\lambda = 1.5\mu\, m$			
	$i = 0$	$i = 1$	$i = 2$
A_i	1.432783	0.002170	-0.000036
B_i	0.063468	-0.007890	0.000147
C_i	-0.415418	0.114257	-0.009127

The effective cladding index n_{FSM} can be used to find the effective *V*-parameter of the CCPCF, treating the CCPCF like a CSF, with its cladding and core indices same as those of

infinite photonic crystal structure and silica, respectively. Now the effective V value of the CCPCF is given by [29, 30, 33, 34]

$$V_{eff} = \frac{2\pi}{\lambda} a_{eff} \left[n_{CO}^2 - n_{FSM}^2 \right]^{1/2} \tag{4}$$

where a_{eff} is the effective core radius which is assumed [29, 30, 33, 34] to be $\Lambda/\sqrt{3}$ and λ is the operating wavelength.

Then using Marcuse formula [31], the modal spot size w_{eff}, half of the mode field diameter (MFD) can be written as [29-31, 35]

$$\frac{w_{eff}}{a_{eff}} = 0.65 + \frac{1.619}{V_{eff}^{3/2}} + \frac{2.879}{V_{eff}^{6}} \tag{5}$$

The spot size of the CCPCF, w_{eff} is obtained by using Eq. (5), where V_{eff} being the effective V-parameter, calculated from Eq. (4). The method of such calculation has been detailed in Appendix A [29, 30].

2.2. Formulation of microlens coupling scheme

The coupling scheme to be studied is shown in Fig. 1. Here, u is the separation distance in between the laser source and the nearest point of the HEML end of the fiber [18-20]. Our analysis is based on some usual approximations [10, 14-20, 22, 23, 26, 27, 29] like Gaussian field distributions for both the source and the fiber, no transmission loss, perfect matching of the polarisation mode of the fiber field, and that on the microlens surface, sufficient angular width of the microlens for ensuring the interception of entire power radiated by the source for typical values of the microlens parameters employed. However, since the spherical aberration is really determined by the properties of the microlens itself, its elimination is difficult by the said adjustment [36].

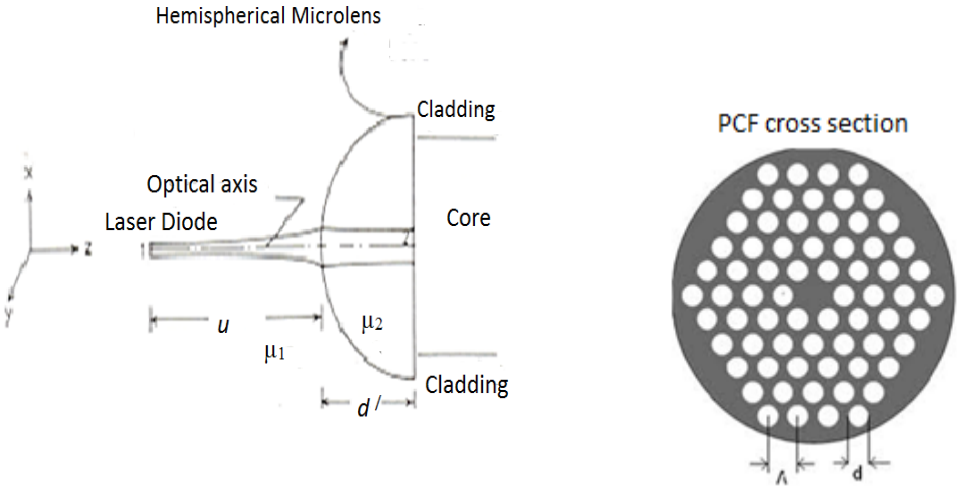

Fig. 1 Geometry of LD to single mode CCPCF coupling via HEML on the tip of the fiber; μ_1 and μ_2 stand for refractive indices of incident and microlens media respectively.

The field Ψ_u representing the output of the LD at a distance u from the HEML surface is expressed by [14-20, 22, 23, 26- 29, 37, 38]

$$\Psi_u = \exp\left[-\left(\frac{x^2}{w_{1x}^2}+\frac{y^2}{w_{1y}^2}\right)\right]\exp\left[-\frac{ik_1}{2}.\frac{x^2+y^2}{R_1}\right] \tag{6}$$

Here, elliptical intensity profiles of the laser beams are approximated by Gaussian spot sizes w_{1x} and w_{1y} along two mutually perpendicular directions, one perpendicular (X) and the other parallel (Y) to the junction planes, k_1 is the wave number in the incident medium and R_1 is the radius of curvature of the wavefronts from the LD. Our analysis is restricted to single frequency laser emitting only one spatial mode with a Gaussian intensity profile.

Moreover, it is already established that Gaussian approximations for the fundamental mode in circular core SMF [14-20, 22, 23, 26, 27, 29] sufficiently represent accurate results in the context of coupling losses for different kinds of microlensing schemes.

The HEML transformed laser field Ψ_v on the fiber plane 2 can be represented by [14-20, 22, 23, 26- 29, 37, 38]

$$\Psi_v = \exp\left[-\left(\frac{x^2}{w_{2x}^2}+\frac{y^2}{w_{2y}^2}\right)\right]\exp\left[-\frac{ik_2}{2}\left(\frac{x^2}{R_{2x}}+\frac{y^2}{R_{2y}}\right)\right] \tag{7}$$

where w_{2x}, w_{2y} are, respectively, microlens transformed spot sizes, R_{2x} , R_{2y} being the respective transformed radii of curvature of the refracted wavefronts in the X and Y directions and k_2 is the wave number in the microlens medium. The method of finding w_{2x}, w_{2y}, R_{2x} and R_{2y} in terms of w_{1x}, w_{1y} and R_1 with the relevant ABCD matrix for HEML on the tip of the fiber is available in literature [18-20] and once again discussed in the Appendix B for ready reference.

The source to fiber coupling efficiency via HEML on the tip of the fiber is expressed in terms of well known overlap integral by [14-20, 22, 23, 26- 29, 37-39]

$$\eta = \frac{\left|\iint \Psi_v \Psi_f^* dxdy\right|^2}{\iint |\Psi_v|^2 dxdy \iint |\Psi_f|^2 dxdy} \tag{8}$$

Therefore η_0, the coupling efficiency in absence of misalignment, for CCPCF is given by [29],

$$\eta_0 = \frac{4w_{2x}w_{2y}w_{eff}^2}{\left[\left(w_{eff}^2+w_{2x}^2\right)^2+\frac{k_2^2 w_{2x}^4 w_{eff}^4}{4R_{2x}^2}\right]^{1/2}\left[\left(w_{2y}^2+w_{eff}^2\right)^2+\frac{k_2^2 w_{2y}^4 w_{eff}^4}{4R_{2y}^2}\right]^{1/2}} \tag{9}$$

However, Eq. (9) can be obtained by employing Eqs. (1) and (7) in Eq. (8).

2.3. Coupling due to allowable aperture

The performance of a HEML is seriously affected due to its limited aperture allowable for transmission of laser beam through it. The radius ρ_c beyond which light transmission is not permitted corresponds to the grazing angle of incidence [18-20] and is shown to be [11],

$$\rho_c = (\mu_1 R_L)/\mu_2, \tag{10}$$

where μ_1 and μ_2 are the refractive indices of the incident and HEML medium respectively, R_L corresponds to the radius of curvature of the HEML.

Accordingly the corrected coupling efficiency η is given as the product of η_0 and the microlens transmittivity factor *T*, where *T* is given by [11, 18-20],

$$T = \frac{\int_0^{\rho_c} \left|\psi_f t\right|^2 rdr}{\int_0^{\infty} \left|\psi_f\right|^2 rdr} \tag{11}$$

and the transmission coefficient (*t*) of the HEML under paraxial approximation is given by

$$t = \frac{2(\mu_1\mu_2)^{0.5}}{\mu_1 + \mu_2}, \tag{12}$$

Thus, the microlens transmittivity factor *T* is obtained by using Eqs. (1) and (10) in Eq.(11) and is given by [18-20]

$$T = t^2[1 - \exp(-2\rho_c^{\,2}/w_{eff}^{\,2})] \tag{13}$$

2.4. Misalignment considerations

An evaluation of the coupling efficiency in the presence of a transverse misalignment in the X-Y plane is based on the assumption that the center of the fiber is displaced to a point having coordinates (d_1,d_2) as shown in Fig. 2.

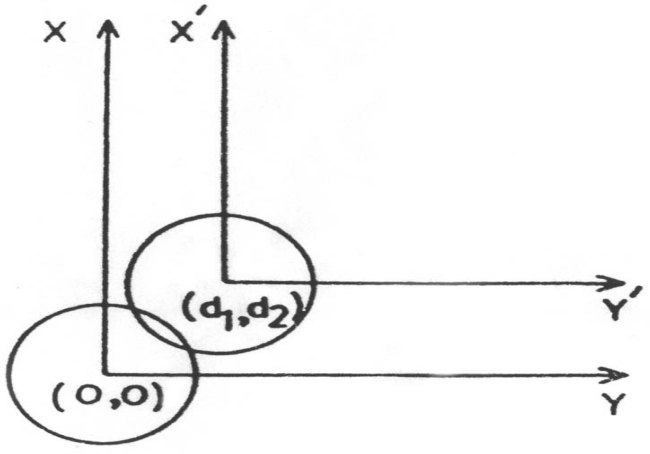

Fig. 2 Transverse misalignment between the imaged laser spot and the center of the fiber

From the well known coordinate transformation technique, the relation between the primed and unprimed coordinates can be given by

$$x = x' + d_1$$
$$y = y' + d_2 \tag{14}$$

In this case, the fundamental mode of the fiber can be represented as [16, 17, 19, 26, 37]

$$\psi_f = \exp\left[-\left(\frac{(x-d_1)^2}{w_{eff}^2} + \frac{(y-d_2)^2}{w_{eff}^2}\right)\right] \tag{15}$$

while the HEML transformed laser field Ψv on the fiber plane 2 can be expressed as already mentioned by Eq. (7).

Employing Eqs. (7) and (15) in Eq. (8), one can obtain the coupling efficiency for only transverse offset as [16, 17, 19, 26, 28]

$$\eta_t = \eta \exp\left[\frac{2d_1^2}{w_{eff}^2}\left\{\frac{w_{2x}^2\left(w_{2x}^2 + w_{eff}^2\right)}{\left(w_{eff}^2 + w_{2x}^2\right)^2 + \frac{k_2^2 w_{2x}^4 w_{eff}^4}{4R_{2x}^2}} - 1\right\}\right] \exp\left[\frac{2d_2^2}{w_{eff}^2}\left\{\frac{w_{2y}^2\left(w_{2y}^2 + w_{eff}^2\right)}{\left(w_{eff}^2 + w_{2y}^2\right)^2 + \frac{k_2^2 w_{2y}^4 w_{eff}^4}{4R_{2y}^2}} - 1\right\}\right] \tag{16}$$

where the corrected coupling efficiency η is given as the product of η_0 and the microlens transmittivity factor *T*, and for CCPCF, η_0, the coupling efficiency in absence of misalignment, is given by Eq.(9).

The angular misalignment of a small angle θ between the HEML and the entrance of the fiber is shown in Fig. 3.

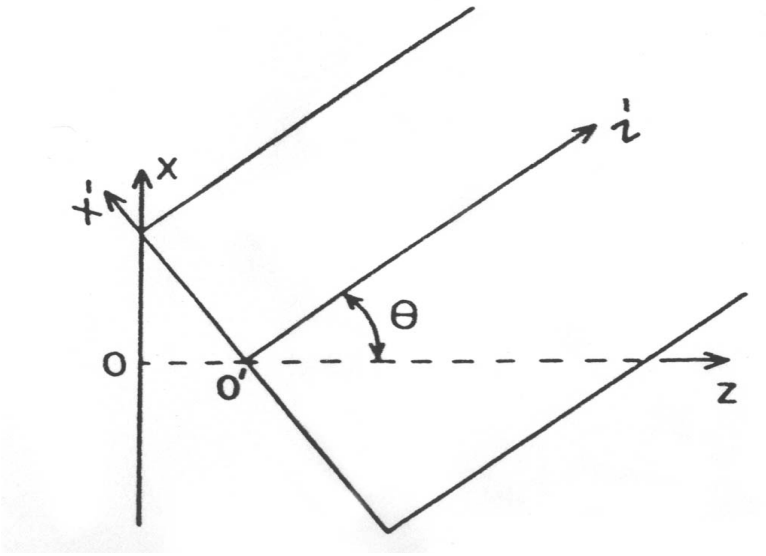

Fig. 3 Angular mismatch between the HEML transformed input face and the end face of the fiber

In such a case the relation between primed and unprimed coordinates is given as

$x = x' \cos\theta + z' \sin\theta$

$y = y'$

$z = -x' \sin\theta + z' \cos\theta$ (17)

We approximate Eq. (17) by using $\sin\theta = \theta$, $\cos\theta = 1$ [28] and $OO' = 0$ for small angular offset (c.f. Fig. 3) and thus obtain

$x = x' + z'\theta$

$y = y'$

$z = -x'\theta + z'$ (18)

The HEML transformed field on the fiber can be given by [16, 17, 19, 26, 28]

$$\Psi_v = \exp\left[-\left(\frac{x^2}{w_{2x}^2} + \frac{y^2}{w_{2y}^2}\right)\right]\exp\left[-\frac{ik_2}{2}\left(\frac{x^2}{R_{2x}} + \frac{y^2}{R_{2y}}\right)\right]\exp(-ik_2 z) \quad (19)$$

Using Eq. (18) and taking care of the fact that at the input end of the fiber z' is zero, one can readily express Eq. (19) in terms of primed coordinates as follows:

$$\Psi_v = \exp\left[-\left(\frac{x'^2}{w_{2x}^2} + \frac{y'^2}{w_{2y}^2}\right)\right]\exp\left[-\frac{ik_2}{2}\left(\frac{x'^2}{R_{2x}} + \frac{y'^2}{R_{2y}}\right)\right]\exp(ik_2 x'\theta) \quad (20)$$

Eqs. (1) and (20) are used in Eq. (8) to obtain the coupling efficiency η_a for a small angular mismatch θ in the case of circular core fiber as mentioned below [16, 17, 19, 26, 28]

$$\eta_a = \eta \exp\left[-\frac{k_2^2\theta^2}{2}\left\{\frac{\left(w_{eff}^2 + w_{2x}^2\right)w_{2x}^2 w_{eff}^2}{\left(w_{eff}^2 + w_{2x}^2\right)^2 + \frac{k_2^2 w_{2x}^4 w_{eff}^4}{4R_{2x}^2}}\right\}\right] \quad (21)$$

Eqs. (16) and (21) can be employed to predict coupling losses for transverse and angular mismatches, respectively.

The above formulations are used in next section to calculate coupling efficiencies in absence and presence of possible transverse and angular misalignments in case of coupling in between LD and. a series of CCPCFs with different air filling ratio d/Λ and lattice constant or hole pitch Λ [29] via HEML of different radii of curvatures [18] on the tip of these fibers.

3. RESULTS AND DISCUSSION

3.1. Optogeometrical parameters under consideration

Taking care of allowable aperture provided by the HEML on the tip of the CCPCF, our formalism employs simple but accurate relevant ABCD matrix under the paraxial approximation in order to predict the coupling optics involving a LD and CCPCF via HEML on the tip of such fiber. For the estimation of coupling efficiencies in absence and presence of any possible transverse and angular misalignments for a HEML of specific radius of curvature [18] on the tip of CCPCF, we firstly use a LD emitting light of wavelength $\lambda = 1.3\mu m$ with

$w_{1x} = 1.081\mu m, w_{1y} = 1.161\mu m$ [12] and then LD emitting light of wavelength $\lambda = 1.5\mu m$ with $w_{1x} = 0.843\mu m, w_{1y} = 0.857\mu m$ [12]. The LD parameters used in this investigation are mentioned in Table 3. For the LD emitting light of abovementioned first wavelength, we study the coupling efficiencies for a series of CCPCFs having different air filling ratio d/Λ and lattice-constant or hole-pitch Λ [29] as mentioned in Table 4. We choose three typical values of d/Λ, in the single moded region ($d/\Lambda \leq 0.45$) corresponding to each arbitrary Λ value (Λ = 2.3, 3.0, 3.5, 4.0, 4.5, 5.0 μm), as 0.35, 0.40, 0.45 [29]. Different fiber spot sizes w_{eff} for these three d/Λ values corresponding to each Λ value (Λ = 2.3, 3.0, 3.5, 4.0, 4.5, 5.0 μm) [29] are then calculated [29, 30] and shown in Table 4 where we also present the relevant working distances (u) with corresponding maximum coupling efficiencies and transmittivity factors for $\lambda = 1.3\mu m$. The idea of transmittivity factor has a relevance as far as the effect of allowable apertures of the HEML is concerned. The values of radii of curvatures (R_L) of the HEML used in this investigation are 6.0, 7.0 μm [18], respectively.

Table 3

Laser diode parameters

LD	Wavelength λ (μm)	Spot size w_{1x} (μm)	Spot size w_{1y} (μm)	λ_1 (μm)	k_2 (μm^{-1})
#1	1.3	1.081	1.161	0.4138	7.4915
#2	1.5	0.843	0.857	0.4775	6.4926

Following [14-20, 22, 23, 26, 27, 29] once again, the refractive index $\mu(=\mu_2/\mu_1)$ of the material of the microlens with respect to surrounding medium is once again taken as 1.55 and thereby the value of transmission coefficient t as found from Eq. (12) is 0.9765 [18-20]. Further, since estimation of coupling efficiency on the basis of planar wave model for the input beam from the LD facet departs slightly from that on the basis of spherical wave model [14-20, 22, 23, 26, 27, 29], we consider planar wave model for the input beam from the LD facet for the sake of simplicity.

Then we use a LD emitting light of wavelength $\lambda = 1.5\mu m$ with $w_{1x} = 0.843\mu m, w_{1y} = 0.857\mu m$ [12]. We compute again relevant working distances with resulting maximum coupling efficiencies for the above same set used in the first part of this investigation and present them in Table 5.

3.2. Results for coupling scheme without misalignment consideration

In order to investigate the coupling optics of LD with CCPCF we have first crosschecked the results with the references dealing with coupling efficiency of a HEML tipped CCSISMF[18] and CCGISMF[20] to LD, for an incident planar wave model. The verification is made by selecting the radii of curvatures, R_L = 6.0 μm and 7.0 μm [18], of the HEML and finding the

optimal coupling efficiencies against effective separation (u) of the LD, emitting light of particular wavelength, from the tip of the microlens.

From Table 4 it is observed that for a fit radius of curvature $R_L = 6.0\ \mu m$ of the HEML the maximum coupling efficiency can reach to 86.88 % (i.e. coupling loss of 0.6108 dB)for a CCPCF with air filling ratio $d/\Lambda = 0.45$, lattice constant $\Lambda = 4.5\mu m$ having respective spot size w_{eff} of 3.236339 μm . The corresponding working distance is 9.7 μm. It is also observed that the coupling efficiencies are optimum for a particular air-filling ratio when we can maintain the ratio of the lattice constant to the air filling ratio as 10. The respective working distances are nearly equal. However, this conclusion of maintaining the ratio of the lattice constant to the air filling ratio cannot be generally drawn for a HEML using radius of curvature $R_L = 7.0\,\mu m$. For radius of curvature $R_L = 7.0\,\mu m$ of the HEML the maximum coupling efficiency is 86.42 % for a CCPCF with air filling ratio $d/\Lambda = 0.45$, lattice constant $\Lambda = 5.0\mu m$ having respective spot size w_{eff} of 3.627302 μm . The corresponding working distance is 11.5 μm.

From Table 5 it is once again observed that for radius of curvature $R_L = 6.0\ \mu m$ of the HEML the maximum coupling efficiency is 68.79 % (i.e. coupling loss of 1.6247 dB) for a CCPCF with air filling ratio $d/\Lambda = 0.40$, lattice constant $\Lambda = 5.0\mu m$ having respective spot size w_{eff} of 4.026105 μm . The corresponding working distance is 10.2 μm. For radius of curvature $R_L = 7.0\ \mu m$ of the HEML the maximum coupling efficiency is 68.20% for a CCPCF with air filling ratio $d/\Lambda = 0.35$, lattice constant $\Lambda = 5.0\mu m$ having respective spot size w_{eff} of 4.490145 μm . The corresponding working distance is 12.0 μm. Thus, from these Tables, it is generally observed that the coupling efficiency can be improved through optimizing simultaneously the working distance and radius of curvature of the HEML. It is also observed from both of these Tables that for a particular air-filling ratio when the lattice constant and hence the fiber spot size increases, the transmittivity factor decreases for a specific radius of curvature of the HEML.

For a typical estimation of knowledge of excitation via HEML with radius of curvature $R_L = 6.0$ μm, excited with LD # 1, 2 emitting light of wavelength $\lambda = 1.3\mu m$ and $\lambda = 1.5\mu m$, respectively we present the variation of coupling efficiencies versus the working distances for fibers corresponding to air filling ratio $d/\Lambda = 0.45$, lattice constant $\Lambda = 4.5\mu m$ having respective spot size w_{eff} of 3.236339 μm and air filling ratio $d/\Lambda = 0.40$, lattice constant $\Lambda = 5.0\mu m$ a having respective spot size w_{eff} of 4.026105 μm as shown in Fig. 4. In this Fig., solid line (_____ denoting EFF0) corresponds to $\lambda = 1.3\mu m$, dashed line (---------- denoting EFF0DS) to $\lambda = 1.5\mu m$. We see that although the values of the typical working distances relevant with the maximum coupling efficiencies corresponding to curves are more or less the same, the optimum coupling efficiency is relatively better observed when the corresponding most suitable CCPCF is excited with LD #1 emitting light of wavelength $\lambda = 1.3\mu m$, in addition to the achievement of the appreciable working distance. However, these values of V_{eff} for light of wavelengths $\lambda = 1.3\mu m$ and $\lambda = 1.5\mu m$, respectively, correspond to low V region which is very well known for evanescent wave coupling in optical fiber directional coupler.

Table 4

Results for optimum coupling efficiency for a series of CCPCFs with different air filling ratio d/Λ and hole-pitch or lattice-constant Λ via HEML with different radii of curvature R_L at operating wavelength $\lambda = 1.3\mu m$. (w_{eff} indicates fiber spot size, u indicates working distance, T indicates transmittivity factor, η_0 indicates coupling coefficient without misalignment and η indicates corrected coupling coefficient without misalignment) $d' = R_L$ (μm), $\mu = 1.55$

d/Λ	Λ (μm)	w_{eff} (μm)	$R_L = 6.0\ \mu m$				$R_L = 7.0\ \mu m$			
			u(μm)	η_0	T	η	u(μm)	η_0	T	η
0.35	2.3	2.475538	7.8	0.8641	0.9464	0.8178	8.1	0.7803	0.9523	0.7431
	3.0	2.744393	8.7	0.9063	0.9357	0.8480	9.4	0.8242	0.9493	0.7824
	3.5	3.071572	9.4	0.9495	0.9138	0.8676	10.5	0.8770	0.9409	0.8252
	4.0	3.482297	10.0	0.9850	0.8730	0.8599	11.3	0.9331	0.9206	0.8590
	4.5	3.957274	10.3	0.9987	0.8129	0.8118	11.8	0.9768	0.8831	0.8626
	5.0	4.433909	10.5	0.9874	0.7459	0.7365	12.2	0.9968	0.8338	0.8311
0.40	2.3	2.106083	5.8	0.8074	0.9524	0.7690	5.4	0.7321	0.9535	0.6980
	3.0	2.422810	7.6	0.8556	0.9478	0.8109	7.8	0.7722	0.9526	0.7357
	3.5	2.740655	8.7	0.9057	0.9359	0.8477	9.4	0.8235	0.9494	0.7819
	4.0	3.121711	9.5	0.9550	0.9095	0.8686	10.6	0.8846	0.9390	0.8307
	4.5	3.553313	10.1	0.9888	0.8647	0.8550	11.4	0.9412	0.9159	0.8620
	5.0	3.985642	10.4	0.9986	0.8090	0.8079	11.9	0.9787	0.8804	0.8616
0.45	2.3	1.859907	3.9	0.7819	0.9534	0.7454	3.0	0.7189	0.9535	0.6855
	3.0	2.191350	6.4	0.8194	0.9517	0.7798	6.1	0.7410	0.9534	0.7064
	3.5	2.493922	7.9	0.8671	0.9458	0.8201	8.2	0.7832	0.9522	0.7458
	4.0	2.845339	9.0	0.9208	0.9300	0.8564	9.8	0.8409	0.9474	0.7966
	4.5	3.236339	9.7	0.9664	0.8990	0.8688	10.8	0.9013	0.9341	0.8419
	5.0	3.627302	10.1	0.9922	0.8558	0.8491	11.5	0.9490	0.9106	0.8642

Table 5

Results for optimum coupling efficiency for a series of CCPCFs with different air filling ratio d/Λ and hole-pitch or lattice-constant Λ via HEML with different radii of curvature R_L, at operating wavelength $\lambda = 1.5\mu m$. (w_{eff} indicates fiber spot size, u indicates working distance, T indicates transmittivity factor, η_0 indicates coupling coefficient without misalignment and η indicates corrected coupling coefficient without misalignment) $d' = R_L$ (μm), $\mu = 1.55$

d/Λ	Λ (μm)	w_{eff} (μm)	$R_L = 6.0\ \mu m$				$R_L = 7.0\ \mu m$			
			u(μm)	η_0	T	η	u(μm)	η_0	T	η
0.35	2.3	2.805033	8.3	0.6364	0.9324	0.5934	8.8	0.5407	0.9482	0.5127
	3.0	2.969228	8.8	0.6679	0.9217	0.6156	9.5	0.5675	0.9442	0.5359
	3.5	3.256532	9.4	0.7234	0.8970	0.6489	10.4	0.6175	0.9332	0.5763
	4.0	3.628935	9.9	0.7918	0.8556	0.6775	11.1	0.6841	0.9105	0.6229
	4.5	4.058139	10.2	0.8608	0.7990	0.6878	11.7	0.7578	0.8734	0.6619
	5.0	4.490145	10.5	0.9164	0.7379	0.6762	12.0	0.8243	0.8275	0.6820
0.40	2.3	2.310718	6.1	0.5527	0.9501	0.5251	5.8	0.4772	0.9531	0.4548
	3.0	2.573870	7.4	0.5942	0.9432	0.5605	7.6	0.5069	0.9515	0.4824
	3.5	2.869064	8.5	0.6486	0.9285	0.6023	9.1	0.5510	0.9468	0.5217
	4.0	3.225618	9.3	0.7175	0.9000	0.6458	10.3	0.6121	0.9346	0.5721
	4.5	3.625593	9.9	0.7912	0.8560	0.6773	11.1	0.6836	0.9107	0.6225
	5.0	4.026105	10.2	0.8562	0.8034	0.6879	11.6	0.7525	0.8766	0.6596
0.45	2.3	1.999448	3.9	0.5204	0.9530	0.4959	3.1	0.4612	0.9535	0.4398
	3.0	2.301137	6.1	0.5514	0.9502	0.5239	5.7	0.4764	0.9531	0.4540
	3.5	2.589569	7.5	0.5970	0.9426	0.5627	7.7	0.5090	0.9514	0.4843
	4.0	2.924104	8.6	0.6592	0.9249	0.6097	9.3	0.5600	0.9455	0.5295
	4.5	3.292278	9.4	0.7302	0.8935	0.6524	10.4	0.6239	0.9314	0.5811
	5.0	3.660019	9.9	0.7973	0.8517	0.6791	11.2	0.6896	0.9082	0.6263

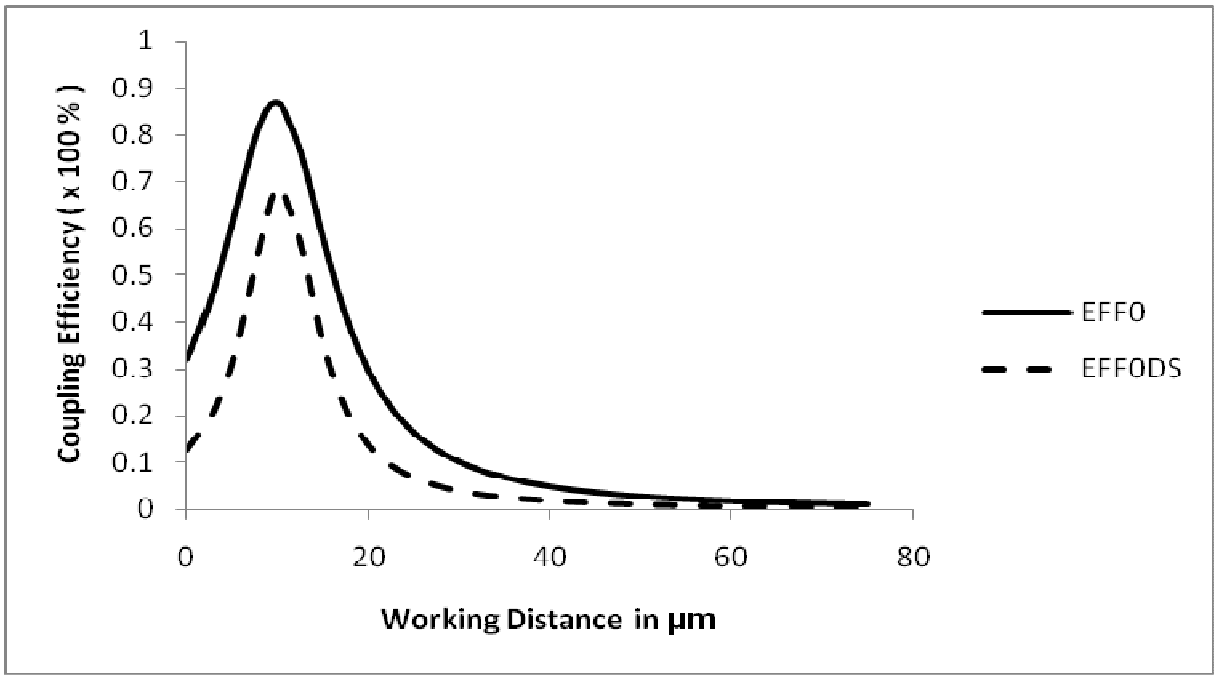

Fig. 4 Variation of coupling efficiency versus working distance for most efficient CCPCF corresponding to $d/\Lambda = 0.45$, $\Lambda = 4.5\mu m$ having w_{eff} of 3.236399 μm, and $d/\Lambda = 0.40$, $\Lambda = 5.0\mu m$ having w_{eff} of 4.026105 μm, excited with LD emitting wavelengths $\lambda = 1.3\mu m$ and $\lambda = 1.5\mu m$, respectively. Solid line (_____ denoting EFF0) corresponds to $\lambda = 1.3\mu m$ and radius of curvature = 6.0 μm, dashed line (---------- denoting EFF0DS) to $\lambda = 1.5\mu m$ and radius of curvature = 6.0 μm.

3.3. Results with misalignment considerations

In our final part, for the computation of the coupling efficiencies in presence of possible transverse and angular mismatches, we use corresponding values of working distances for most suitable CCPCFs with air filling ratio $d/\Lambda = 0.45$, lattice constant $\Lambda = 4.5\mu m$ having spot size w_{eff} of 3.236339 μm and air filling ratio $d/\Lambda = 0.40$, lattice constant $\Lambda = 5.0\mu m$ having spot size w_{eff} of 4.026105 μm for excitement by LD #1, 2, respectively. The results corresponding to transverse and angular mismatches are reported in Table 6. These investigations of coupling efficiencies are restricted around 0 to 2 μm region for transverse offset and 0 to 2^0 region for angular offset [16, 17, 19, 26]. This region is chosen so that the designers of microlenses can restrict the fabrication to such small mismatches.

Table 6

Coupling efficiencies with transverse and angular misalignments for most efficient CCPCF with a specific air filling ratio d/Λ and hole pitch or lattice constant Λ via HEML with a specific radius of curvature R_L excited with LD #1 & LD #2, respectively. (w_{eff} indicates fiber spot size, u indicates working distance, η indicates corrected coupling coefficient without misalignment, η_{10}^{*} indicates coupling coefficient for transverse misalignment of 2 μm along X direction only while η_{01}^{*} indicates coupling coefficient for transverse misalignment of 2 μm along Y direction only, η_{a}^{*} represents coupling coefficient for angular misalignment of 2^0 and CL indicates corresponding coupling loss) $d' = R_L$ (μm), $\mu = 1.55$

$\lambda = 1.3\ \mu m$					$\lambda = 1.5\ \mu m$				
$d/\Lambda = 0.45$, $\Lambda = 4.5\ \mu m$, $w_{eff} = 3.236339\ \mu m$					$d/\Lambda = 0.40$, $\Lambda = 5.0\ \mu m$, $w_{eff} = 4.026105 \mu m$				
$R_L = 6.0\ \mu m$					$R_L = 6.0\ \mu m$				
$u(\mu m)$	η and CL_0 (dB)	η_{10}^{*} and CL_{10}^{*} (dB)	η_{01}^{*} and CL_{01}^{*} (dB)	η_{a}^{*} and CL_{a}^{*} (dB)	$u(\mu m)$	η and CL_0 (dB)	η_{10}^{*} and CL_{10}^{*} (dB)	η_{01}^{*} and CL_{01}^{*} (dB)	η_{a}^{*} and CL_{a}^{*} (dB)
9.7	0.8688 0.6108	0.6362 1.9642	0.6219 2.0624	0.4448 3.5180	10.2	0.6879 1.6247	0.5864 2.3183	0.5845 2.3321	0.2774 5.5684

From Table 6, it is evident that coupling efficiencies corresponding to transverse and angular misalignments show mutually complemental results. It must be noted in Table 6 that the symbol η_{10}^{*} indicates coupling coefficient for transverse misalignment of 2 μm along X direction only while η_{01}^{*} indicates coupling coefficient for transverse misalignment of 2 μm along Y direction only. On the other hand, η_{a}^{*} represents coupling coefficient for angular mismatch of 2^0. Now, the calculated no offset value of coupling loss for the most efficient fiber with air filling ratio $d/\Lambda = 0.45$, lattice constant $\Lambda = 4.5 \mu m$ having respective spot size w_{eff} of 3.236339 μm excited with LD #1 emitting light of wavelength $\lambda = 1.3 \mu m$ is obtained as 0.6108 dB. Further, it is evident from the same Table that the calculated coupling losses for this fiber is 1.9642 dB for transverse misalignments of 2 μm along X direction only while the calculated coupling loss for this specific fiber is 2.0624 dB for transverse misalignments of 2 μm along Y direction only. It is also observed that the coupling losses for the said fiber is 3.5180 dB for angular mismatch of 2^0. On the other hand, the calculated no offset value of coupling loss for the most efficient fiber with air filling ratio $d/\Lambda = 0.40$, lattice constant $\Lambda = 5.0 \mu m$ having respective spot size w_{eff} of 4.026105 μm excited with LD #2 emitting light of wavelength $\lambda = 1.5 \mu m$ is obtained as 1.6247 dB. Further, it is evident from Table 6 that the calculated coupling losses for this fiber is 2.3183

dB for transverse misalignments of $2\,\mu m$ along X direction only while the calculated coupling loss for this specific fiber is 2.3321 dB for transverse misalignments of $2\,\mu m$ along Y direction only. It is also found that the coupling losses for the said fiber is 5.5684 dB for angular mismatch of 2^0. It is observed that the concerned coupling efficiency for transverse misalignment along X direction is always marginally higher than that for the transverse misalignment along Y direction Moreover, with the increase of angular offset the coupling efficiency decreases relatively faster than that for those obtained with increasing transverse offset as far as comparison of coupling efficiencies from no offset value is concerned. However, as the transverse mismatch is more sensitive than that of angular mismatch, the results for CCPCF with air filling ratio $d/\Lambda = 0.45$, lattice constant $\Lambda = 4.5\mu m$ and respective spot size w_{eff} of 3.236339 μm are most suitable when excited with LD #1 emitting light of wavelength $\lambda = 1.3\mu m$.

Then, for the typical estimation of knowledge of excitation by LDs emitting light of wavelengths $\lambda = 1.3\mu m$ and $\lambda = 1.5\mu m$, to the most suitable CCPCF with air filling ratio $d/\Lambda = 0.45$, lattice constant $\Lambda = 4.5\mu m$ having respective spot size w_{eff} of 3.236339 μm and air filling ratio $d/\Lambda = 0.40$, lattice constant $\Lambda = 5.0\mu m$ having respective spot size w_{eff} of 4.026105 μm via HEML of radius of curvature = $6.0\mu m$ on its tip in presence of possible transverse misalignments, we present the variation of coupling efficiencies versus the transverse misalignments in Figs. 5 and 6, respectively. The coupling efficiency designated as EFF10 is represented by the dashed line (corresponding to $d_2 = 0$ with d_1 varying from 0 to $2\,\mu m$) while the coupling efficiency EFF01 is represented by the solid line (corresponding to $d_1 = 0$ with d_2 varying from 0 to $2\,\mu m$). In Figs. 7 and 8, the curves present the variation of coupling efficiencies with the angular mismatch for the said fiber excited with LDs emitting light of wavelength $\lambda = 1.3\mu m$ and $\lambda = 1.5\mu m$, respectively.

In CSFs, the single-mode optical bandwidth is typically limited by macro-bend loss at long wavelengths and a higher-order mode cutoff at short wavelengths [40]. The endlessly single-mode property of the PCF [8] has the specious consequence that the waveguide can be scaled to an arbitrary dimension while remaining single mode [40]. Moreover, the PCF is observed to have a significantly larger bandwidth than the CSF of an identical MFD as per as the measurements of the spectral attenuation, single-turn bend loss etc. are concerned [40]. It is observed in our present analysis that, for an identical fit radius of curvature of 6.0 μm of HEML on the tip CCPCFs with specific air filling ratio and hole pitch, the maximum coupling efficiency can reach to 86.88 % for the working distance $u = 9.7\ \mu m$ in case of excitement by a LD emitting light of wavelength $\lambda = 1.3\mu m$ while the optimized value of the coupling efficiency is only 68.79 % for the working distance $u = 10.2\ \mu m$ in case of excitement by a LD emitting light of wavelength $\lambda = 1.5\mu m$. Consequently the coupling losses, both in absence and presence of possible misalignments, have been reduced for excitement by a LD emitting light of wavelength $\lambda = 1.3\mu m$ in comparison with that obtained for excitement by a LD emitting light of wavelength $\lambda = 1.5\mu m$. Moreover, it is mentioned in Ref. [41] that the additional design

parameters of hole diameter, *d,* and hole-to-hole spacing, Λ in PCF, enable much greater flexibility in the design of dispersion to suit the required application while in CSFs, group velocity dispersion is usually dominated by the dispersion of the bulk silica. Thus, our present analysis and results point out the merit of CCPCFs with specific air filling ratio and lattice constant in coupling by a LD emitting specially light of wavelength $\lambda = 1.3\mu m$ via HEML of specific radius of curvature on the tip of such fiber. Although there is a limitation of availability of experimental research papers in the field of microlens coupling involving CCPCFs, we are fortunate enough to compare our proposed results with those mentioned in the available literature [42] for the paraboloidal-shaped microlens etched from an SMF and fused on PCF having MFD of 11.1 μm excited by a LD of wavelength 1.31 μm. It is observed that our presented coupling scheme is in excellent agreement with those results mentioned in Ref. [42]. Thus, with the advent of new progress in nanotechnology, we are optimistic that the future technologist, will involve any breakthrough to reduce the dispersion values, related with the wavelength 1.3 μm, by further optimization of the structure and better control of the fluctuations in fiber diameter and, ultimately realize and test our results of the above proposed theoretical formalism experimentally in near future.

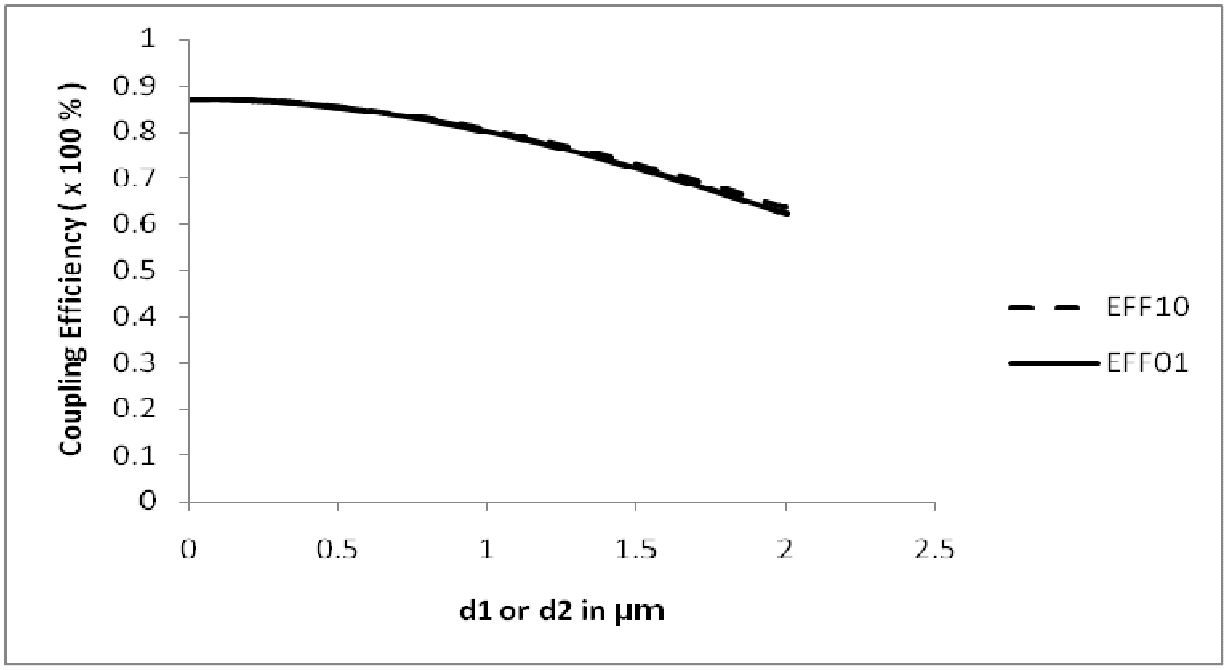

Fig. 5 Variation of coupling efficiencies with the transverse misalignment for most efficient CCPCF having $d/\Lambda = 0.45$, $\Lambda = 4.5\mu m$ and w_{eff} of 3.236399 μm excited with LD emitting wavelength $\lambda = 1.3\mu m$. The coupling efficiency designated as EFF10 is represented by the dashed line (corresponding to $d_2 = 0$ with d_1 varying from 0-2 μm) while the coupling efficiency EFF01 is represented by the solid line (corresponding to $d_1 = 0$ with d_2 varying from 0-2 μm).

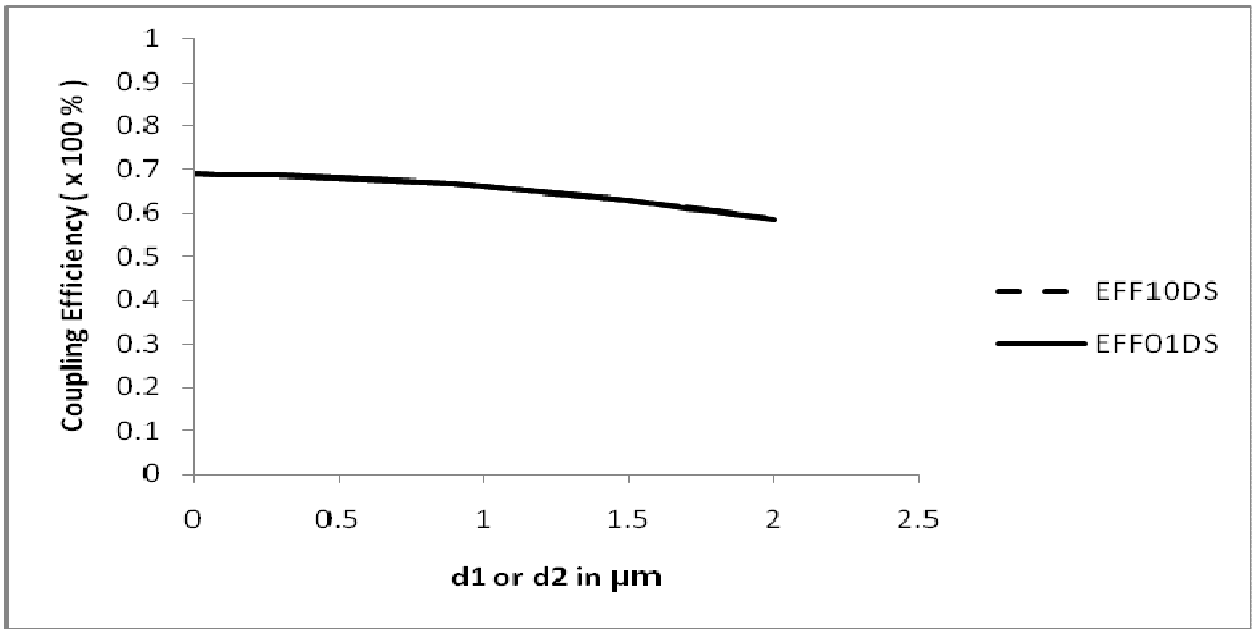

Fig. 6 Variation of coupling efficiencies with the transverse misalignment for most efficient CCPCF having $d/\Lambda = 0.40$, $\Lambda = 5.0\mu m$ and w_{eff} of 4.026105 μm excited with LD emitting wavelength $\lambda = 1.5\mu m$. The coupling efficiency designated as EFF10DS is represented by the dashed line (corresponding to $d_2 = 0$ with d_1 varying from 0-2 μm) while the coupling efficiency EFF01DS is represented by the solid line (corresponding to $d_1 = 0$ with d_2 varying from 0-2 μm).

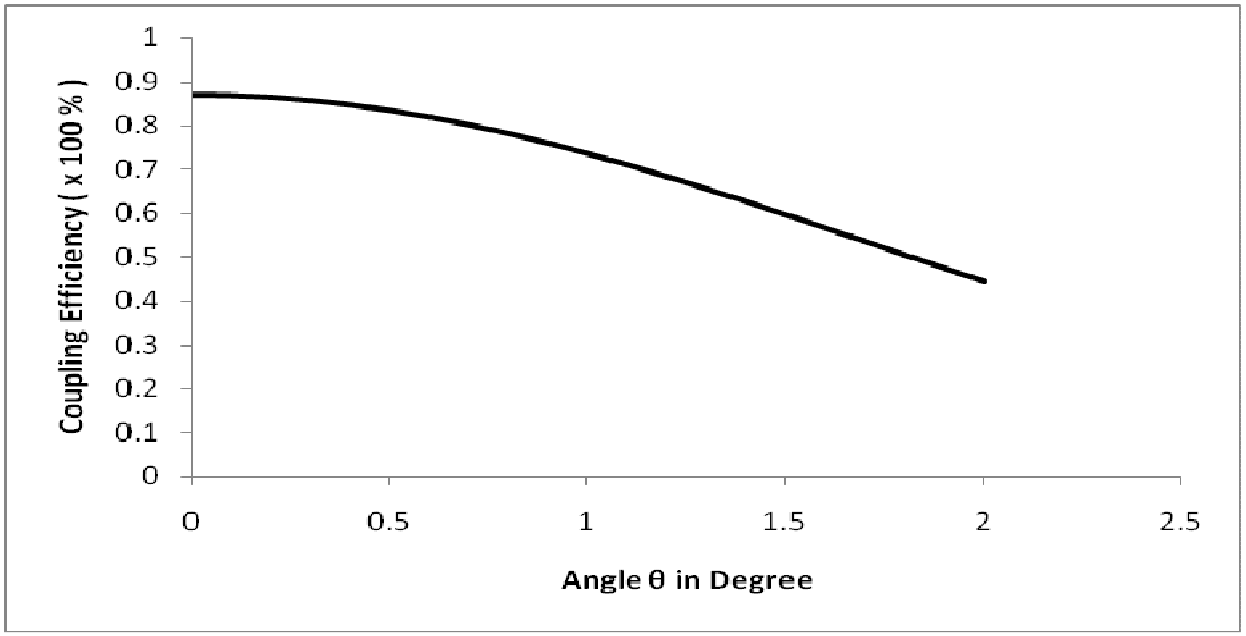

Fig. 7 Variation of coupling efficiency with the angular misalignment for most efficient CCPCF having $d/\Lambda = 0.45$, $\Lambda = 4.5\mu m$ and w_{eff} of 3.236399 μm excited with LD emitting wavelength $\lambda = 1.3\mu m$.

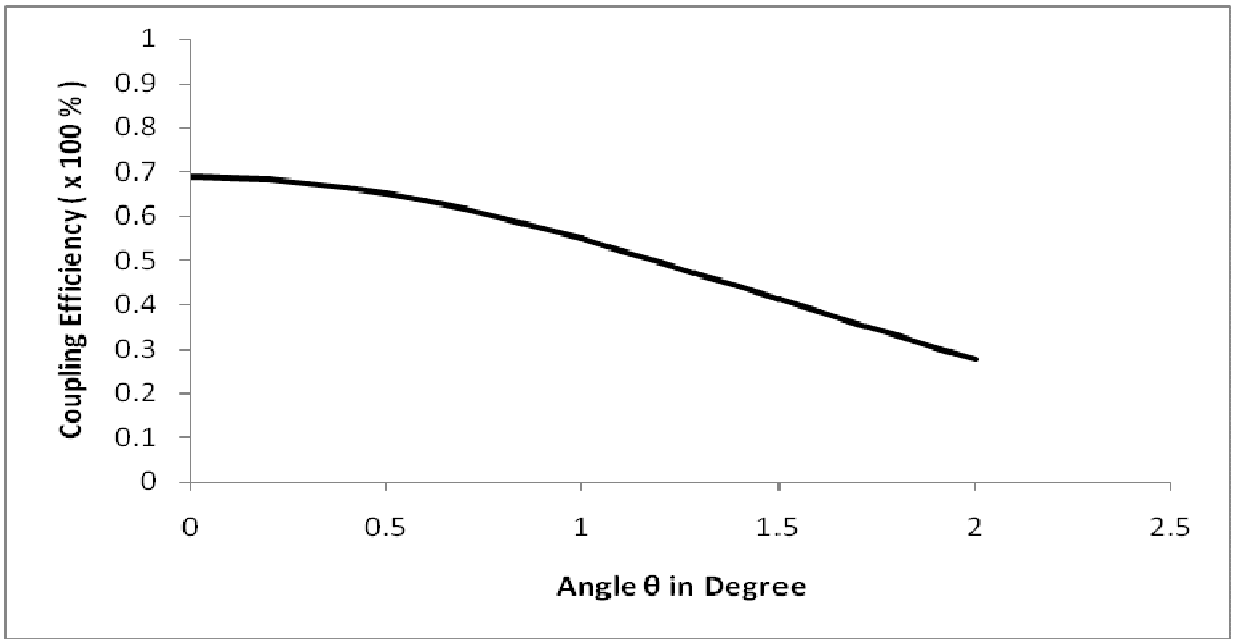

Fig. 8 Variation of coupling efficiency with the angular misalignment for most efficient CCPCF having $d/\Lambda = 0.40$, $\Lambda = 5.0\mu m$ and w_{eff} of 4.026105 μm excited with LD emitting wavelength $\lambda = 1.5\mu m$.

4. CONCLUSION

Employing ABCD matrix for refraction by a HEML of different radii of curvature on the tip of a series of CCPCFs with different air filling ratio d/Λ and lattice constant Λ, we present, for the first time, to the best of our knowledge, a simple but realistic method for evaluation of coupling efficiency for LD to CCPCF coupling in absence and presence of possible transverse and angular mismatches. The best maximum coupling with optimisation of appropriate working distance is achieved for a CCPCF with air filling ratio of 0.45 and lattice constant of 4.5 μm when excited with LD emitting light of wavelength $\lambda = 1.3\mu m$. Further, the importance of achieving longest working distance to have maximum coupling efficiency also stands in favour of the said CCPCF. Moreover the optimized values of the radius of curvature R_L= 6.0 μm of the HEML are playing a crucial role in both cases. In comparison with the other deeply involved rigorous methods like FDM and FEM, the application of novel ABCD matrix has simplified the analysis as the concerned calculations need very little mathematical calculations. The method is also realistic in the sense that it takes care of the allowable aperture of such microlens. Moreover, the method predicts acceptable air filling ratio and lattice constant of the CCPCF from the point of view of fabrication of HEML of allowable practical radius of curvature. The technique developed should be useful in the system designing and packaging of suitable HEML in coupling optics. The results are also extremely useful for assessing deeply the sensitivity of the coupler with reference to two kinds of mismatches. However, the designers and packagers should be more careful in order to avoid angular mismatches as is visualized that a little angular misalignment causes a pronounced setback in comparison with little transverse misalignment.

Appendix A

The usual normalized parameters u and v for the infinite cladding region of the chosen CCPCF are given by [2, 29, 30]

$$u = k\Lambda\left(n_{CO}^2 - \frac{\beta^2}{k^2}\right)^{1/2} \tag{A1}$$

and

$$v = k\Lambda\left(n_{CO}^2 - 1\right)^{1/2} \tag{A2}$$

with

$$u^2 + w^2 = v^2 . \tag{A3}$$

In order to obtain the effective cladding index n_{FSM}, a basic air-hole at the centre of a hexagonal unit cell is approximated to a circle in a regular photonic crystal [8, 29, 30]. Then from relevant boundary conditions for the fields and their derivatives in terms of appropriate special functions, corresponding to a fixed value of v, obtained from Eq. (A2) for fixed Λ and λ-values, the concerned u values are computed for different d / Λ values at a particular λ from the following Eq., taking n_{CO} = 1.45 [2, 29, 30]

$$\begin{aligned} &wI_1(a_n w)\left[J_1(bu)Y_0(a_n u) - J_0(a_n u)Y_1(bu)\right] \\ &+uI_0(a_n w)\left[J_1(bu)Y_1(a_n u) - J_1(a_n u)Y_1(bu)\right] = 0 \end{aligned} \tag{A4}$$

where $a_n = \frac{d}{2\Lambda}$, $b = \left(\frac{\sqrt{3}}{2\pi}\right)^{1/2}$.

Using Eq. (A4), Russell has provided a polynomial fit to u, only for $d/\Lambda = 0.4$ and n_{CO} = 1.444. Further, for all d/Λ values of practical interest in the endlessly single mode region of a CCPCF, where d/Λ is less than 0.45, one should have a more general equation for wide applications [30].

The values of n_{FSM} are determined by replacing β/k in Eq. (A1) with n_{FSM} and this will lead to a modified simpler formulation of n_{FSM} as [29, 30]

$$n_{FSM} = A + B\left(\frac{d}{\Lambda}\right) + C\left(\frac{d}{\Lambda}\right)^2 \tag{A5}$$

where A, B and C are the three different optimization parameters, dependent on both the hole-pitch Λ and the relative hole-diameter or hole-size d/Λ.

Since optical communication window corresponds with two operating wavelengths of 1.3 μm and 1.5 μm, this study finds the coefficients for these two wavelengths of practical interest for different possible hole-pitches and hole-sizes of the CCPCF. Such modification in such a fitting is advantageous in the sense that it will help to reduce computation time since only nine coefficients are required in calculation instead of twenty seven coefficients [29, 30].

Now, for each value of Λ with the variations of d/Λ, the n_{FSM} values corresponding to respective u values obtained from Eq. (A4) are determined. Applying least square fitting of n_{FSM} in terms of d/Λ to Eq. (A5) for a particular Λ, the values of A, B and C can be then estimated. The various values of A, B and C are then simulated for different Λ in the endlessly single mode region of the CCPCF, resulting in the empirical relations of A, B and C in Eq. (A5), in terms of Λ, as expressed in the following [29, 30]

$$A = A_0 + A_1\Lambda + A_2\Lambda^2 \tag{A6}$$

$$B = B_0 + B_1\Lambda + B_2\Lambda^2 \tag{A7}$$

$$C = C_0 + C_1\Lambda + C_2\Lambda^2 \tag{A8}$$

where A_i, B_i and C_i ($i = 0,1$ and 2) are the optimization parameters for A, B and C, respectively. Computing A, B and C from Eqs. (A6-A8), one can find n_{FSM} directly for any d/Λ and Λ value at any particular λ using Eq. (A5) in the endlessly single mode region of the CCPCFs.

Appendix B

The input and output parameters (q_1, q_2) of the light beam is given as

$$q_2 = \frac{Aq_1 + B}{Cq_1 + D} \tag{B1}$$

where

$$\frac{1}{q_{1,2}} = \frac{1}{R_{1,2}} - \frac{i\lambda_0}{\pi w_{1,2}^2 \mu_{1,2}} \tag{B2}$$

The ray matrix M for the HEML under consideration on the tip of CCPCF is expressed as [18-20]

$$M = \begin{pmatrix} A & B \\ C & D \end{pmatrix}$$

$$M = \begin{pmatrix} 1 & d' \\ 0 & 1 \end{pmatrix} \begin{pmatrix} 1 & 0 \\ \dfrac{1-\mu}{\mu R_L} & \dfrac{1}{\mu} \end{pmatrix} \begin{pmatrix} 1 & u \\ 0 & 1 \end{pmatrix} \tag{B3}$$

where,

$$A = 1 + \frac{d'(1-\mu)}{\mu R_L}$$

$$B = u + \frac{(1-\mu)ud'}{\mu R_L} + \frac{d'}{\mu}$$

$$C = \frac{1-\mu}{\mu R_L}$$

$$D = \frac{1}{\mu} + \frac{(1-\mu)u}{\mu R_L} \tag{B4}$$

are the matrix components, expanded according to (B3).

The parameter d' is the maximum width of the HEML and is equal to the radius of curvature R_L of the concerned microlens. u is the distance separating the tip of the microlens from the LD.

Again, the refractive index of the material of the HEML with respect to the surrounding medium is represented by $\mu(=\mu_2/\mu_1)$. The transformed beam spot sizes and radii of curvature in the X and Y directions are obtained by using Eqs. (B4) in Eqs. (B1) and (B2) and can be expressed as

$$w_{2x,2y}^2 = \frac{A_1^2 w_{1x,1y}^2 + \dfrac{\left(\lambda_1^2 B^2\right)}{w_{1x,1y}^2}}{\mu(A_1 D - BC_1)} \tag{B5}$$

$$\frac{1}{R_{2x,2y}} = \frac{A_1 C_1 w_{1x,1y}^2 + \dfrac{\left(\lambda_1^2 BD\right)}{w_{1x,1y}^2}}{A_1^2 w_{1x,1y}^2 + \dfrac{\left(\lambda_1^2 B^2\right)}{w_{1x,1y}^2}} \tag{B6}$$

where

$$\lambda_1 = \frac{\lambda}{\pi},\ \lambda = \frac{\lambda_0}{\mu_1},\ A_1 = A + \frac{B}{R_1} \quad \text{and} \quad C_1 = C + \frac{D}{R_1}. \tag{B7}$$

In plane wavefront model, the radius of curvature R_1 of the wavefront from the laser facet $\rightarrow\infty$. This leads to $A_1 = A$ and $C_1 = C$.

REFERENCES

[1] P. St. J. Russell, "Photonic crystal fibers", Science, **299**(5605), 358-362 (2003)

[2] P. St. J. Russell, "Photonic-crystal fibers", J. Lightwave Technol., **24**(12), 4729–4749 (2006)

[3] A. Bjarklev, J. Broeng, and A. S. Bjarklev, *Photonic Crystal Fibres*, (Springer Science & Business Media Inc., NewYork, 2003)

[4] R. Bhattacharya, and S. Konar, "Extremely large birefringence and shifting of zero dispersion wavelength of photonic crystal fibers", Opt. & Laser Technol., **44,** 2210–2216 (2012)

[5] M. Sharma, N. Borogohain, and S. Konar, "Index Guiding Photonic Crystal Fibers With Large Birefringence and Walk-Off", J. Lightwave Technol., **31,** 3339-3344 (2013)

[6] R. Bhattacharya, and S. Konar, "Design of a Photonic Crystal Fiber with Zero Dispersion Wavelength Near 0.65 μm", Fiber and Integrated Opt., **27,** 89–98 (2008)

[7] M. Sharma, S. Konar, and K. R. Khan, "Supercontinuum generation in highly nonlinear hexagonal photonic crystal fiber at very low power", J. Nanophotonics, **9,** 093073(1-8) (2015)

[8] T. A. Birks, J. C. Knight, and P. St. J. Russell, "Endlessly single-mode photonic crystal fiber", Opt. Lett., **22**(13), 961-963 (1997)

[9] E. Li, "Characterization of fiber lens", Opt. Lett., **31**, 169-171 (2006)
[10] H. M. Presby, and C. A. Edwards, "Near 100% efficient fibre microlenses", Electron. Lett., **28**, 582-584 (1992)
[11] C. A. Edwards, H. M. Presby, and C. Dragone, "Ideal microlenses for laser to fiber coupling", J. Lightwave Technol., **11**, 252-257 (1993)
[12] J. John, T. S. M. Maclean, H. Ghafouri-Shiraz, and J. Niblett, "Matching of single-mode fibre to laser diode by microlenses at 1.5 μm wavelength", IEE Proc. Optoelectron., **141**, 178-184 (1994)
[13] H. M. Presby, and C. A. Edwards, "Efficient coupling of polarization maintaining fiber to laser diodes", IEEE Photon. Technol. Lett., **4**, 897-899 (1992)
[14] S. Gangopadhyay, and S.N. Sarkar, "Laser diode to single-mode fibre excitation via hyperbolic lens on the fibre tip: Formulation of ABCD matrix and efficiency computation", Opt. Commun., **132**, 55-60 (1996)
[15] S. Gangopadhyay, and S. N. Sarkar, "ABCD matrix for reflection and refraction of Gaussian light beams at surfaces of hyperboloid of revolution and efficiency computation for laser diode to single-mode fiber coupling by way of a hyperbolic lens on the fiber tip", Appl. Opt., **36**, 8582-8586 (1997)
[16] S. Gangopadhyay, and S. N. Sarkar, "Misalignment considerations in laser diode to single-mode fibre excitation via hyperbolic lens on the fibre tip", Opt. Commun., **146**, 104-108 (1998).
[17] S. Mukhopadhyay, and S. N. Sarkar, "Coupling of a laser diode to single mode circular core graded index fiber via hyperbolic microlens on the fiber tip and identification of the suitable refractive index profile with consideration for possible misalignments", Opt. Eng., **50**(4), 045004(1-9) (2011)
[18] S. Gangopadhyay, and S. N. Sarkar, "Laser diode to single-mode fiber excitation via hemispherical lens on the fiber tip: Efficiency computation by ABCD matrix with consideration for allowable aperture", J. Opt. Commun., **19**, 42-44 (1998)
[19] S. Gangopadhyay, and S. N. Sarkar, "Misalignment considerations in laser diode to single-mode fiber excitation via hemispherical lens on the fiber tip", J. Opt. Commun., **19**, 217-221 (1998)
[20] A. Bose, S. Gangopadhyay, and S. C. Saha, "Laser diode to single mode circular core graded index fiber excitation via hemispherical microlens on the fiber tip: Identification of suitable refractive index profile for maximum efficiency with consideration for allowable aperture", J. Opt. Commun., **33**(1), 15-19 (2012)
[21] H. Liu, L. Liu, R. Xu, and Z. Luan, "ABCD matrix for reflection and refraction of Gaussian beams at the surface of a parabola of revolution", Appl. Opt., **44**, 4809-4813 (2005)
[22] H. Liu, "The approximate ABCD matrix for a parabolic lens of revolution and its application in calculating the coupling efficiency", Optik, **119**, 666-670 (2008)
[23] S. Mukhopadhyay, "Coupling of a laser diode to single mode circular core graded index fiber via parabolic microlens on the fiber tip and identification of the suitable refractive index profile with consideration for possible misalignments", J. Opt., **45**(4), 312–323 (2016)

[24] G. A. Massey, and A. E. Siegman, "Reflection and refraction of Gaussian light beams at tilted ellipsoidal surfaces", Appl. Opt., **8,** 975-978 (1969)
[25] S. K. Mondal, S. Gangopadhyay, and S. N. Sarkar, "Analysis of an upside-down taper lens end from a single-mode step index fiber", Appl. Opt., **37**, 1006-1009 (1998)
[26] S. K. Mondal, and S. N. Sarkar, "Coupling of a laser diode to single-mode fiber with an upside-down tapered lens end", Appl. Opt., **38**, 6272-6277 (1999)
[27] S. Mukhopadhyay, "Laser diode to circular core graded index single mode fiber excitation via upside down tapered microlens on the fiber tip and identification of the suitable refractive index profile", J. Phys. Sci., **20**, 173-187 (2015)
[28] A. K. Ghatak, and K. Thyagarajan, *Optical Electronics*, (Cambridge University Press, United Kingdom, 1998) Ch. 13, p 411-415
[29] A. Karak, D. Kundu, S. Mukhopadhyay, and S. N. Sarkar, "Investigation of coupling of a laser diode to photonic crystal fiber via hyperbolic microlens on the fiber tip by ABCD matrix formalism", Opt. Eng., **54**(8)**,** 086102(1-7) (2015)
[30] D. Kundu, and S. Sarkar, "Prediction of propagation characteristics of photonic crystal fibers by a simpler, more complete and versatile formulation of their effective cladding indices", Opt. Eng., **53**(5), 056111(1-6) (2014)
[31] D. Marcuse, "Loss analysis of single-mode fiber splices", J. Bell Syst. Tech., **56**(5), 703–718 (1977)
[32] T. Hirooka, Y. Hori, and M. Nakazawa, "Gaussian and sech approximations of mode field profiles in photonic crystal fibers", IEEE Photon. Technol. Lett., **16,** 1071-1073 (2004)
[33] M. Koshiba, and K. Saitoh, "Applicability of classical optical fiber theories to holey fibers", Opt. Lett., **29**(15), 1739–1741 (2004)
[34] K. Saitoh, and M. Koshiba, "Empirical relations for simple design of photonic crystal fibers", Opt. Express **13(**1), 267-274 (2005)
[35] A. K. Ghatak, and K. Thyagarajan, *Introduction to Fiber Optics*, (Cambridge University Press, United Kingdom, 1998)
[36] M. Bass, and V. N. Mahajan, *Handbook of Optics, in Geometrical and Physical Optics, Polarised Light, Components and Instruments*, Vol**. 1**. 3rd edn. (McGraw-Hill, NewYork, 2010) Chapters 22 and 29
[37] S. N. Sarkar, K. Thyagarajan, and A. Kumar, "Gaussian approximation of the fundamental mode in single mode elliptic core fibers", Opt. Commun., **49**, 178-183 (1984)
[38] S. N. Sarkar, B. P. Pal, and K. Thyagarajan, "Lens coupling of laser diodes to monomode elliptic core fibers", J. Opt. Commun., **7**, 92-96 (1986)
[39] J. Sakai, and T. Kimura, "Design of miniature lens for semiconductor laser to single mode fiber coupling", IEEE J. Quantum Electron., **QE-16,** 1059–1066 (1980)
[40] M. D. Nielsen, J. R. Folkenberg, N. A. Mortensen, and A. Bjarklev, "Bandwidth comparison of photonic crystal fibers and conventional single mode fibers", Opt. Express, **12**(3), 430-435 (2004)

[41] W. H. Reeves, J. C. Knight, P. St. J. Russell, and P. J. Roberts, "Demonstration of ultra-flattened dispersion in photonic crystal fibers", Opt. Express, **10 (**14), 609- 613 (2002)
[42] Z. S. Peng, and L. Wang, "Optical coupling between a lensed photonic crystal fiber and a laser diode", *Int. Conf. on Communications, Circuits and Systems*, Guilin, (IEEE, Guilin, 2006)